Firing Correlations Improve Detection of Moving Bars
IJCNN 2003

Garrett T. Kenyon
P-21, MS D454
Los Alamos National Laboratory (LANL)
Los Alamos, NM 87545

James Theiler
NIS-2, MS D436
LANL
Los Alamos, NM 87545

David W. Marshak
Neurobiology & Anatomy
Univ. of Texas Med. Sch.
Houston, TX 77030

Bartlett Moore
Neurobiol. & Anat.
U. of TX Med Sch.
Houston, TX

Janelle Jeffs
Bioengineering
U. of UT
Salt Lake City, UT

Bryan J. Travis
EES-2, MS T003
LANL
Los Alamos, NM

***Abstract*-Moving stimuli elicit oscillatory responses from retinal ganglion cells at frequencies between 60-100 Hz. We used a computer model of the inner retina to investigate whether the additional firing synchrony resulting from stimulus-evoked high frequency oscillations could contribute to the detection of moving bars. The responses of the model ganglion cells were similar to those of cat alpha cells. Event trains from the model ganglion cells stimulated by moving bars were summed into a threshold detector with a short integration window (2-4 msec) whose output was classified by an ideal observer. To isolate the contribution from firing correlations, the model ganglion cells were replaced by independent Poisson generators with matched time-dependent event rates. Compared to this control, firing correlations between the model ganglion cells allowed for improved detection of moving stimuli.**

I. INTRODUCTION

The detection of moving stimuli presents a difficult problem for the visual system. A narrow low-contrast bar, 1 degree across and moving at 40 degrees of visual angle per second, excites a retinal ganglion cell with a 1 degree receptive field center for only 25 msec, producing at best only a few extra spikes above baseline. Despite the difficulty involved, the reliable detection of fast moving stimuli is of clear behavioral relevance and it is likely that special mechanisms have evolved to facilitate this process. One mechanism that might be used by the retina to detect rapidly moving stimuli is to synchronize the underlying neural responses. Alpha ganglion cells in the cat retina exhibit high-frequency oscillations that are tightly phased locked among cells responding to the same moving bar, with a temporal precision of a few msecs (1; 2). Based on their ability to respond to high velocities (3), alpha ganglion cells are thought to mediate the perception of rapidly moving stimuli.

We used a computer model of the inner mammalian retina to investigate the oscillatory responses of alpha ganglion cells evoked by narrow moving bars presented at a range of velocities and intensities. Our goal was to see whether the firing correlations between ganglion cells predicted by the retinal model could be utilized to detect a moving bar more reliably than would be possible using information from the firing rates alone. To extract the information encoded by oscillatory retinal output, we employed a threshold element with a short integration time (2-4 msec). This detection strategy is consistent with studies showing that synchrony between retinal ganglion cells propagates to the visual cortex (4) and with reports that neurons in cat primary visual cortex are differentially selective to synchronous inputs arriving within a few msec of each other (5).

Stimulus coordination from a moving bar will also produce some synchrony between co-activated ganglion cells in addition to that resulting from intrinsic retinal interactions. We controlled for synchrony due to stimulus coordination by repeating the analysis using independent Poisson generators with the same time-dependent event rates as the model ganglion cells, but lacking the synchronous, high frequency oscillations resulting from feedback interactions in the inner retina. Our findings suggest that by synchronizing their responses via high frequency oscillations, retinal ganglion cells make rapidly moving stimuli more readily detectable.

II. METHODS

Computer Model: There were five distinct cell types in the retinal model (fig. 1). All cell types were modeled as single compartment, RC circuit elements obeying a first order differential equation of the following form:

$$\dot{\vec{V}}^{(k)} = \frac{1}{\tau^{(k)}}\left(\vec{V}^{(k)} - \sum_{k'}\vec{W}^{(k,k')} \cdot f^{(k,k')}\left(\vec{V}^{(k')}\right) \cdot \vec{W}^{(k,k')^T} - b^{(k)} - \vec{L}^{(k)}\right)$$

where $\{V^{(k)}\}$ are the membrane potentials of cells of type k (curly brackets denote the elements of the corresponding matrix), $\tau^{(k)}$ is the time constant, $b^{(k)}$ is the resting potential, $\{L^{(k)}\}$ represents light stimulation, $\{W^{(k,k')}\}$ gives the connection strengths between presynaptic, k', and postsynaptic, k, cell types as a function of their vertical (or horizontal) separation, and the functions $f^{(k,k')}$ are input-output relations, detailed below. Axonal conduction velocity was

0-7803-7898-9/03/$17.00 ©2003 IEEE

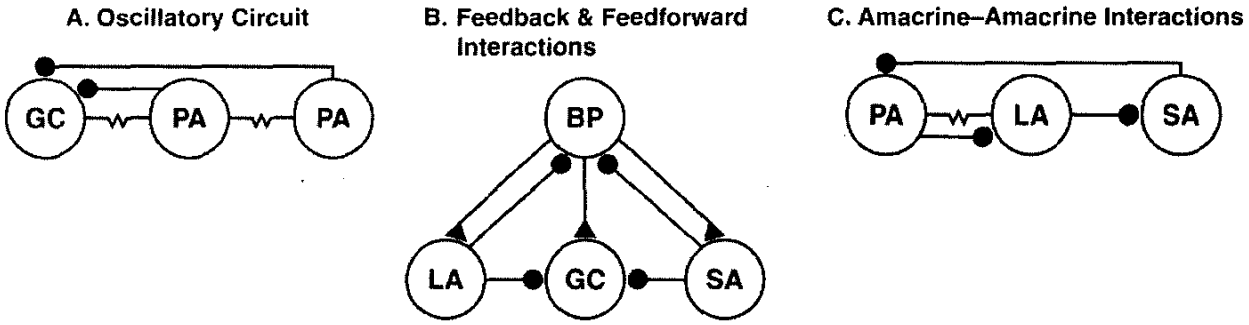

Fig. 1. Connectivity. There were 5 cells types, bipolar (BP) cells, small (SA), large (LA) and poly-axonal (PA) amacrine cells, and ganglion (GC) cells, the latter arranged as a 32x32 square mosaic. a) The PAs were electrically coupled to each other and to the GCs. The PA axons made feedback inhibitory synapses onto the GCs and PAs, as well as weaker synapses onto the other cell types (not shown). b) The BPs provided local excitation to the SAs, LAs, and the GCs (triangles). The SAs and LAs provided local feedback inhibition to the BPs and local feed forward inhibition to the GCs. c) Serial inhibition. The three amacrine cells types made local serial inhibitory synapses among themselves, producing a negative feedback loop.

3.5 GC receptive field diameters per msec plus a fixed synaptic delay equal to 1 msec. The time step was 1 msec, as control experiments showed that using an Euler integration method the model exhibited qualitatively similar behavior independent of step-size.

The input-output function for gap junctions was given by the identity:

$$f^{(k,k')}\left(\tilde{V}^{(k')}\right) = \tilde{V}^{(k')}$$

where the dependence on the presynaptic potential has been absorbed into the definition of $\tau^{(k)}$. The input-output function for non-spiking synapses was constructed by comparing, on each time step, a random number with a Fermi-function:

$$f^{(k,k')}\left(\tilde{V}^{(k')}\right) = \theta\left(\left[1+\exp\left(-\alpha\tilde{V}^{(k')}\right)\right]^{-1} - r\right)$$

where α sets the gain, r is a uniform random deviate between 0 and 1, and θ is a step function, $\theta(x) = 0$, $x \le 0$; $\theta(x) = 1$, $x > 0$. The input-output relation used for spiking synapses was:

$$f^{(k,k')}\left(\tilde{V}^{(k')}\right) = \theta\left(\tilde{V}^{(k')} - \tilde{T}^{(k')}\right),$$

where $\{T^{(k')}\}$ denotes the threshold value for each neuron. For spiking cells, a positive pulse was applied after the membrane potential crossed threshold, followed by a negative pulse on the next time step. The threshold was incremented following each spike, and then decayed back to zero with the time constant of the cell.

In the horizontal direction, synaptic strengths fell off as Gaussian functions of the distance between the pre- and post-synaptic cells:

$$W^{(k,k')}_{i^{(k)},j^{(k')}} = z\sqrt{W^{(k,k')}}\exp\left[-\left\|i^{(k)} - j^{(k')}\right\|^2 \Big/ 2\sigma^2\right]$$

where $W^{(k,k')}_{(i(k),j(k'))}$ is the weight factor from the presynaptic cell $j(k')$ (located in the j^{th} column in the array of cells of type k') to the postsynaptic cell $i(k)$, z is a normalization factor that ensured the total synaptic input equaled $W^{(k,k')}$, σ is the Gaussian radius, and the quantity $\|i(k)-j(k')\|$ denotes the horizontal distance between the pre- and postsynaptic cells, taking into account the wrap around boundary conditions employed to mitigate edge effects. An analogous weight factor described the dependence on vertical separation. Synapses were non-zero only if the output radius of the presynaptic cell overlapped the input radius of the postsynaptic cell. Except for axonal connections, the input and output radii were the same for all cell types.

III. RESULTS

The responses of the model ganglion cells to moving bars resembled those of cat alpha cells (3). The firing rate, measured by the PSTH, increased from low to moderate velocities and then declined at higher velocities (fig. 2, histograms). In the model, peak-firing rates increased at moderate velocities because local inhibition from the non-spiking amacrine cells was slower than the central excitation. However, the amplitude of the central excitatory drive was also limited by the low-pass filter characteristics of the model bipolar and ganglion cells, leading to reductions in the peak firing rate at the highest velocities tested.

The PSTHs were smoothed to remove high-frequency oscillations that were time-locked to the stimulus. At higher velocities, such oscillations can be seen superimposed on the broader response to the bar itself. To remove these high frequency oscillations, we applied a low pass filter with a sharp cutoff at 50 Hz. The smoothed PSTH was multiplied by a scale factor to ensure that the total area under the peak (499-531 msec) remained unchanged. The peak firing rates, as estimated by the

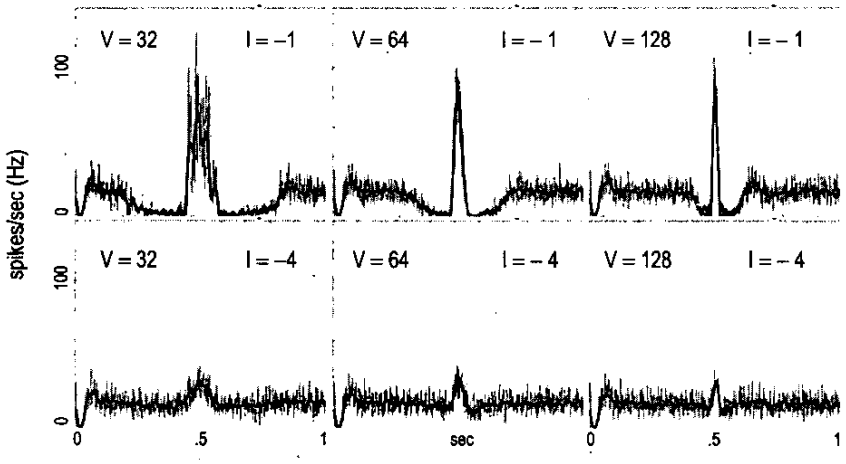

Fig. 2. Velocity tuning. Narrow bars, covering a 1×8 array of ganglion cells, were moved across the retina at various speeds and intensities. PSTHs constructed from 100 stimulus presentations (bin width, 2 msec). Smoothed line obtained by low pass filtering and equalizing the total peak area. Velocity units are pixels/sec.

smoothed PSTHs, were used to construct velocity-tuning curves (fig. 3). These were qualitatively similar to the velocity-tuning curves recorded from cat alpha cells (3), in that there was a peak velocity at which responses were maximal. Differences from the velocity-tuning curve measured experimentally are most likely due to the absence of an outer plexiform layer in our retinal model, which would have supplied additional low pass temporal filtering and contrast gain control.

High intensity moving bars elicited oscillatory responses at frequencies of approximately 90 Hz that synchronized the stimulated ganglion cells with a temporal precision of several msecs. To assess the synchronous, high-frequency oscillations between the model ganglion cells evoked by moving bars, cross-correlation-histograms (CCHs) were constructed between pairs of ganglion cells stimulated by the opposite ends of the moving bars (fig. 4, left panels). The high frequency oscillations present in the CCHs were not readily visible in the raw PSTH (see fig. 2), as the oscillations were not strongly phase locked to the stimulus onset and thus averaged out over multiple stimulus trials. The expected CCH due to stimulus coordination, or shift-predictor (fig. 4, dashed lines), was non-negligible at high velocity but correlation strength continued to increase even after stimulus-locked correlations were subtracted (fig 4, solid lines). Comparing synchrony, integrated power between 40-160 Hz, and firing rate, with all three quantities measured relative to their respective baselines, we found that oscillations were modulated over the largest dynamic range as a function of bar velocity. The synchrony increased as a function of bar velocity at speeds greater than 8 pixels/sec, but the average firing rate during the response peak was relatively insensitive to the rate of motion. In the following, we ask whether the synchronous, oscillatory responses evoked by moving bars could contribute to the detection of such stimuli.

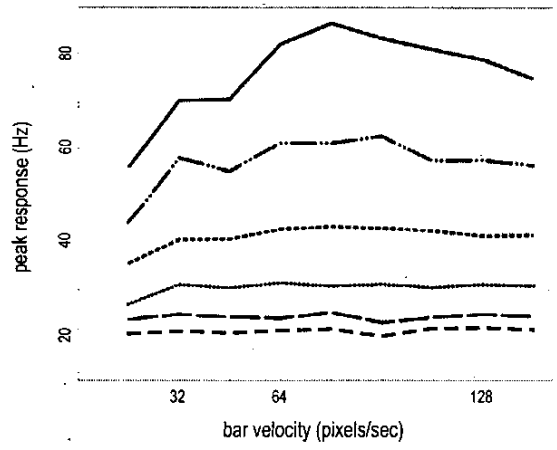

Fig. 3. Velocity tuning curves. Peak firing rate vs. bar velocity was plotted for a 32-fold range of stimulus intensities (−6 to −1 in $\log_2$ units).

The oscillatory responses generated by the model ganglion cells made it easier to detect moving bars against the background activity when using a threshold process with a short integration time window. Spikes from a line of eight ganglion cells activated by a narrow bar were summed into a threshold detector (fig. 5, illustration). The event rate of the detector was determined by the total number of supra-threshold inputs occurring during a 32 msec time window centered on the response peak. To calibrate the detector, the detection threshold was adjusted to yield a baseline event rate of approximately 1 Hz.

During the passage of a moving bar, inhibitory feedback from electrically coupled amacrine cells caused ganglion cell responses to oscillate. To assess the extent to which the detector was able to utilize these synchronous oscillations, the eight stimulated ganglion cells were replaced by independent Poisson generators whose time-dependent firing rates were determined by the smoothed

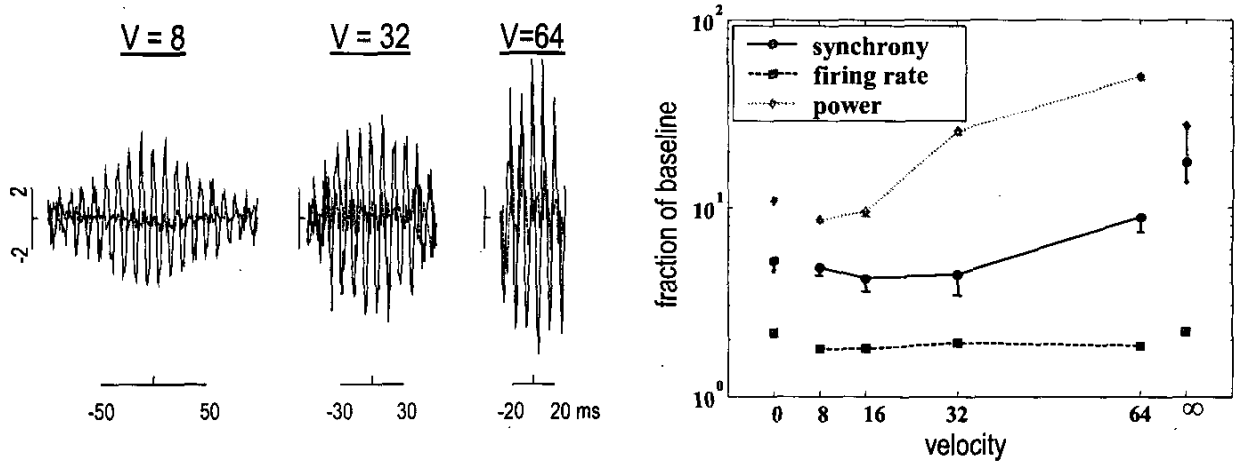

Fig. 4. Firing correlations are modulated by stimulus velocity. Left: Ganglion cell oscillations produced by different velocities (top, pixels/sec). Cross-Correlation-Histograms (CCHs) between pairs of ganglion cells stimulated by opposite ends of the bar. Firing correlations (solid) increased in amplitude with increasing velocity even after the shift predictor was subtracted (dashed). Right: The integrated power in the gamma band (40-160 Hz, dotted-diamonds) was more strongly modulated by stimulus velocity than either the synchrony (solid-circles) or average firing rate (dashed-squares). All quantities measured relative to their respective baselines.

PSTHs. Thus, the Poisson control incorporated firing correlations due to stimulus coordination, but lacked the precise temporal information arising from the lateral interactions in the retinal model. The passage of the bar produced a greater increase in the detector event rate when the inputs were correlated by synchronous, high-frequency oscillations than when the inputs were independent (fig. 5, panels). This extra sensitivity was due to the fact that a threshold process is well suited for detecting synchronous events (6; 7), a property also exhibited by cortical neurons (5).

An ideal observer was used to analyze the distributions of detector events recorded during both the passage and absence of a moving bar, yielding an estimate of the fraction of stimulus presentations that could be correctly classified, relative to baseline, on single trials

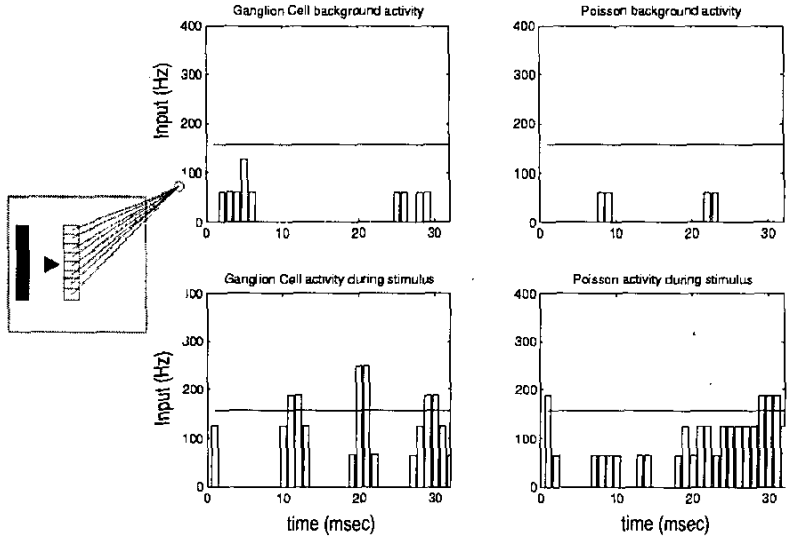

Fig. 5. Threshold detection. Illustration: Spike trains from 8 ganglion cells activated by a moving bar were summed into a threshold detector (time window, 2 msec). Left Column: Model ganglion cells. Right: Independent Poisson generators with matched time-dependent event rates. Top Row: Baseline activity. Bottom Row: Stimulated activity. Oscillations produced additional suprathreshold events.

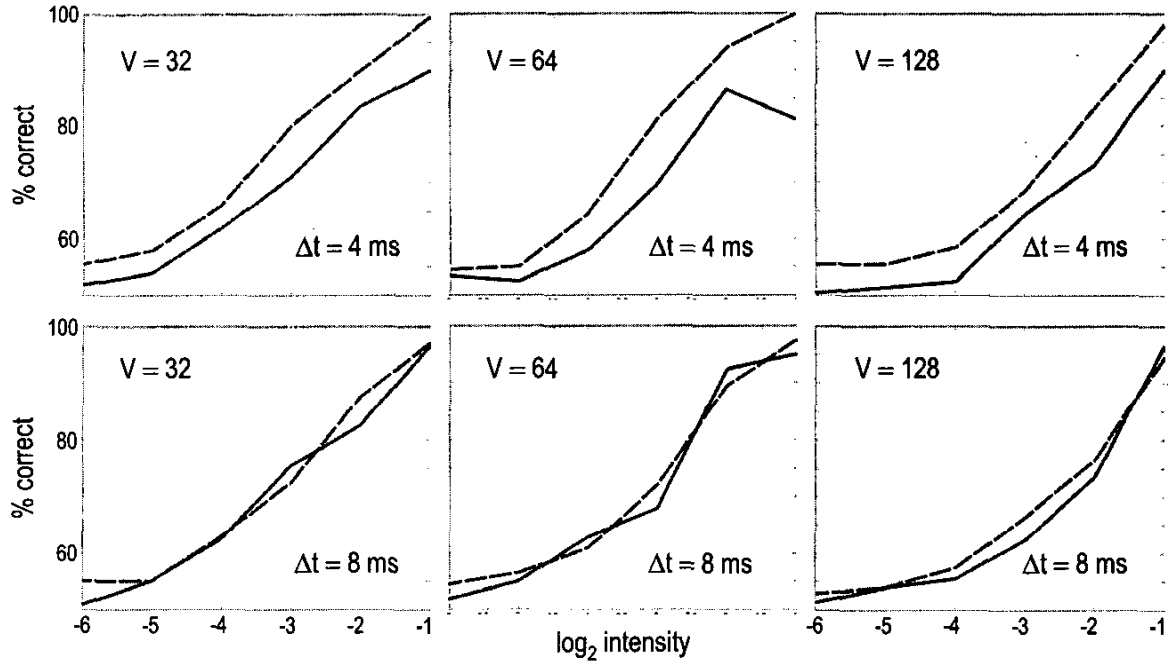

Fig. 6. Ideal observer. The distribution of detection events produced by moving bars (V=32,64,128 pixels/sec, left to right columns, respectively) was compared to the baseline event distribution, and their overlap used to estimate the fraction of stimulus presentations detected by an ideal observer. Synchrony between the model ganglion cells (dashed) led to improved performance on the bar detection task compared to the Poisson control (solid) when the integration time window of the threshold detector was 4 msec (top row), but not 8 msec (bottom row).

(fig. 6, top row). Compared to the Poisson control, correlations between the model ganglion cells produced a greater number of detection events at each bar intensity, which in turn made the corresponding event distributions more separable. Thus, for most stimulus intensities and velocities tested, the output of the threshold detector could be classified more reliably than when the same detector was driven by independent sources.

The improved detectability of moving stimuli requires a decoding process that is sensitive to firing correlations between retinal ganglion cells with temporal precision of less than 5 msecs. To assess the effect of integration window size on the ability to extract information from synchronously firing neurons, the ideal observer analysis was repeated using threshold detectors with summation window of 8 msecs. With the longer summation window, high frequency oscillations no longer led to superior performance compared to the Poisson control. With a long integration time, the synchrony between the model ganglion cells could not be resolved by the threshold process, and thus firing synchrony with msec precision was no longer advantageous.

IV. DISCUSSION

Oscillatory responses between 60-100 Hz are seen in extracellular recordings of the responses of retinal ganglion cells to large stimuli (1; 2; 8) and in the primate ERG (9). Given this experimental evidence, we asked what information processing function high frequency oscillations might serve. One possibility is that synchronous oscillations contribute to image segmentation. Oscillatory responses of cat retinal ganglion cells can be strongly feature selective; that is, ganglion cell pairs responding to the same high contrast stimulus synchronize their firing activity, yet fire in an uncorrelated fashion when responding to separate stimuli (1). However, for relative phase to uniquely encode connectedness, the degree of phase locking should be independent of stimulus velocity, which might otherwise confound the interpretation of synchronous input. Yet our results indicate that oscillations increase with stimulus velocity, as in the cat (2). Thus, rather than playing a central role in segmentation, the primary function of synchronous oscillations may be to convey other information about the stimulus.

Here, we have shown that oscillatory responses of ganglion cells allow moving stimuli to be detected more reliably than would be the case if each ganglion cell fired independently. A coincidence detector based on a simple threshold process performed better on a moving bar detection task as a result of synchronous oscillations between the model ganglion cells. This performance advantage was measured relative to a control that replaced the output of the model retina with independent Poisson spike trains

possessing matched time-dependent event rates. This effect required a detector with a short integration time, and this is consistent with studies showing that visual neurons can respond as coincidence detectors with integration times on the order of a few msec (5).

In an earlier study based on a linear model, we provided evidence that gap junctions with axon-bearing amacrine cells provide a feedback pathway within the retina that could generate oscillatory light responses (10). When a group of ganglion cells were depolarized, they depolarized the axon-bearing amacrine cells that were electrically coupled to them. The ganglion cells were all hyperpolarized by the ensuing wave of axon-mediated inhibition, and then repolarized together to initiate the next cycle of the oscillation. The synaptic connections that generate oscillatory responses in the model are consistent with known retinal anatomy, but our conclusions are applicable regardless of the mechanism that generates oscillations.

For rapidly moving bars, synchrony resulting from stimulus coordination might be expected to overwhelm any additional synchrony due to intrinsic retinal mechanisms, but we have shown stimulus coordination does not confound the contribution from high-frequency oscillations. Because the synchrony due to stimulus coordination is of lower temporal precision, a threshold detector with a short time constant can be used to isolate the contribution from retinal oscillations. However, there is no need to differentiate between synchronous spikes due to stimulus coordination and those due to retinal oscillations. Indeed, the synchrony from these two sources can simply be added together in order to improve detection. These findings suggest that the function of firing correlations is to increase the probability of responses in the postsynaptic neurons.

Averaging over many stimulated ganglion cells is one way to obtain an accurate estimate of their mean firing rate, but this requires that the individual neurons be statistically independent (11). Strong correlations, on the other hand, make it more difficult to extract information encoded by the mean firing rate of a group of ganglion cells. However, our results suggest that the information lost due to correlations can be offset by the enhanced reliability of detection, provided the information is decoded by a threshold process with a brief integration window. We propose that, under some circumstances, the visual system may sacrifice some information capacity in order to detect stimuli more reliably.

Acknowledgments

Supported by the NIH, the DOE LDRD program, and the MIND Institute.

References

1. **Neuenschwander S and Singer W**. Long-range synchronization of oscillatory light responses in the cat retina and lateral geniculate nucleus. *Nature* 379: 728-732, 1996.

2. **Neuenschwander S, Castelo-Branco M and Singer W**. Synchronous oscillations in the cat retina. *Vision Res* 39: 2485-2497, 1999.

3. **Cleland BG and Harding TH**. Response to the velocity of moving visual stimuli of the brisk classes of ganglion cells in the cat retina. *Journal of Physiology* 345: 47-63, 1983.

4. **Castelo-Branco M, Neuenschwander S and Singer W**. Synchronization of visual responses between the cortex, lateral geniculate nucleus, and retina in the anesthetized cat. *J Neurosci* 18: 6395-6410, 1998.

5. **Alonso JM, Usrey WM and Reid RC**. Precisely correlated firing in cells of the lateral geniculate nucleus. *Nature* 383: 815-819, 1996.

6. **Kenyon GT, Fetz EE and Puff RD**. Effects of firing synchrony on signal propagation in layered networks. In: *Advances in Neural Information Processing Systems 2*, edited by Touretzky DS. San Mateo: Morgan Kaufmann, 1990, p. 141-148.

7. **Kenyon GT, Puff RD and Fetz EE**. A general diffusion model for analyzing the efficacy of synaptic input to threshold neurons. *Biol Cybern* 67: 133-141, 1992.

8. **Ishikane H, Kawana A and Tachibana M**. Short- and long-range synchronous activities in dimming detectors of the frog retina. *Vis Neurosci* 16: 1001-1014, 1999.

9. **Frishman LJ, Saszik S, Harwerth RS, Viswanathan S, Li Y, Smith EL, 3rd, Robson JG and Barnes G**. Effects of experimental glaucoma in macaques on the multifocal ERG. Multifocal ERG in laser-induced glaucoma. *Doc Ophthalmol* 100: 231-251, 2000.

10. **Kenyon GT and Marshak DW**. Gap junctions with amacrine cells provide a feedback pathway for ganglion cells within the retina. *Proc R Soc Lond B Biol Sci* 265: 919-925, 1998.

11. **Shadlen MN and Newsome WT**. The variable discharge of cortical neurons: implications for connectivity, computation, and information coding. *J Neurosci* 18: 3870-3896, 1998.